JOURNAL OF COMPUTATIONAL PHYSICS 44, 302–317 (1981)

Boundary Conditions Which Lead to Excitation of Instabilities in Plasma Simulations

DANIEL W. SWIFT AND JOHN J. AMBROSIANO

Geophysical Institute, University of Alaska, Fairbanks, Alaska 99701

Received June 16, 1981

Two examples of two-dimensional electrostatic particle-code simulations are shown in which one exhibits characteristics of a stable plasma while the other exhibits unstable, long wavelength plasma oscillations. The only difference between the two simulations is a change in the boundary condition on the electrostatic potential. An energy theorem is derived which shows that the rate of change of field and particle energy within a closed volume is related to a surface integral involving the electrostatic potential and the normal component of the electric current. An analytic theory is developed for a one-dimensional plasma to show how boundary effects can excite spurious plasma instabilities. The theory is tested with a series of one-dimensional plasma simulations. Finally, practical considerations on means of avoiding the non-physical instabilities in simulation plasmas are given.

1. INTRODUCTION

A tool of growing importance in understanding the kinetic processes within a plasma is computer particle simulation. In this computational algorithm, the paths of hundreds of thousands of particles are followed as they move in self-consistent and externally applied electromagnetic fields. The self-consistent fields are calculated at sample points on a grid using the particle positions and velocities. The forces from the fields are then interpolated at the particle positions to advance the particles to the next time-step, and the cycle is repeated to the end of the calculation.

Since the very beginning of this method, the primary concern has been to reproduce the essential behavior of a real plasma while avoiding non-physical phenomena due solely to the limitations of the numerical method. An obvious requirement is that the simulation of a theoretically stable plasma should also be stable. This is not always easy to achieve. The requirement of stability has led investigators to a number of well-known design considerations, e.g.: the size of the time-step in relation to the highest natural frequency, the size of the Debye length as compared with the cell dimensions, and so on [1].

Recently, another aspect of simulation design has been of some concern, namely, the handling of boundaries. A sizable majority of plasma simulations have used periodic boundaries. This is an appropriate choice for modelling an infinite,

0021-9991/81/120302–16$02.00/0

homogeneous plasma. Periodicity also enables one to use fast Fourier transform (FFT) techniques, which are quite efficient to solve the equations for the fields. The FFT method also provides ready access to information about the time-development of Fourier modes, which helps to match linear plasma theory to plasma simulation. Particle trajectories in this case are necessarily periodic as well, and if one keeps the usual rules regarding time-steps and grid spacing, the periodic simulation is relatively trouble-free. However, it is often necessary to model finite plasmas, or to include boundary effects. For example, a problem of interest in studies of the earth's magnetosphere is to simulate the voltage drop along magnetic field lines due to current-driven shock formation in the region between the ionosphere and the magnetosphere [2]. The ionosphere is conveniently represented as a conducting endplate, while the field lines in the magnetosphere are taken to be equipotentials. This means that in the solution of Poisson's equation for the potential, ϕ, at one end of the domain ϕ must satisfy the boundary condition $\phi(z=0)=0$, while at the other end $\partial\phi/\partial z|_{z=L}=0$ is imposed. The field lines are taken to be vertical (z-axis), and periodic boundary conditions in the horizontal direction can be assumed.

In two-dimensional problems where boundary conditions are imposed along two opposing ends of a domain, fast Fourier transform (FFT) methods can be used in the horizontal, x, direction where periodic boundary conditions can be imposed. Efficient finite difference methods, which incorporate boundary conditions, can be used to calculate solutions for the z-dependence of each Fourier mode. Recently, Decyk and Dawson [3] have proposed a method that makes use of the FFT in two directions, and also makes it possible to add solutions of Laplace's equation to the doubly periodic solutions of Poisson's equation to obtain solutions which satisfy prescribed boundary conditions in both directions.

However, boundary conditions imposed on a simulation plasma may have unintended effects on the plasma. For example, Decyk and Dawson [3] report considerable differences in the degree to which energy is conserved in a plasma, depending on whether zero potential conditions or vacuum boundary conditions are assumed, with the latter showing much poorer energy conservation. In addition, problems can arise due to the way particles are handled at the boundaries. In a situation in which a magnetic field is tangential to a boundary, Naitou *et al.* [4] have shown that some methods for reflecting particles at boundaries [5] result either in particle density gradients or boundary currents. When the magnetic field is highly oblique to the boundary, boundary currents have been shown to excite drift waves whose effects propagate into the interior of the plasma.

In our attempts to model a bounded plasma we have observed the development of large-amplitude instabilities, with no apparent physical cause. The conditions of whether or not an instability will be excited and the growth rate appear to be quite sensitive to boundary conditions on both the electrostatic potential and on the particles. To illustrate boundary effects, we show the results of two two-dimensional simulations of bounded plasmas, one giving the appearance of stability and the other exhibiting unstable behavior. Both plasmas consist of 32,768 ions and electrons, with an ion to electron mass ratio of 100. The electrons were assumed to be strongly

magnetized, constrained to follow magnetic field lines in the z-direction, while the ions were left completely unmagnetized. Both species have equal temperatures, and both drift at two-thirds the electron thermal speed in the negative z-direction. The electron Debye length is two grid units, in a plane defined by 128×128 grid points. Only the electrostatic interaction was included. The Poisson equation was solved by Fourier transform methods in x and finite difference methods in z. Also in the calculations, the $k_\perp = 0$ mode was suppressed. Both runs had periodic particle boundary conditions in x, that is, a particle that crossed a boundary was inserted in the opposite boundary. Particles that crossed boundaries normal to the magnetic field were also reinserted at the opposite ends, but the velocities were reinitialized.

Figure 1 shows equipotential contours at 10 electron plasma periods into a run in which the potential was set to zero along the top and bottom boundaries of the

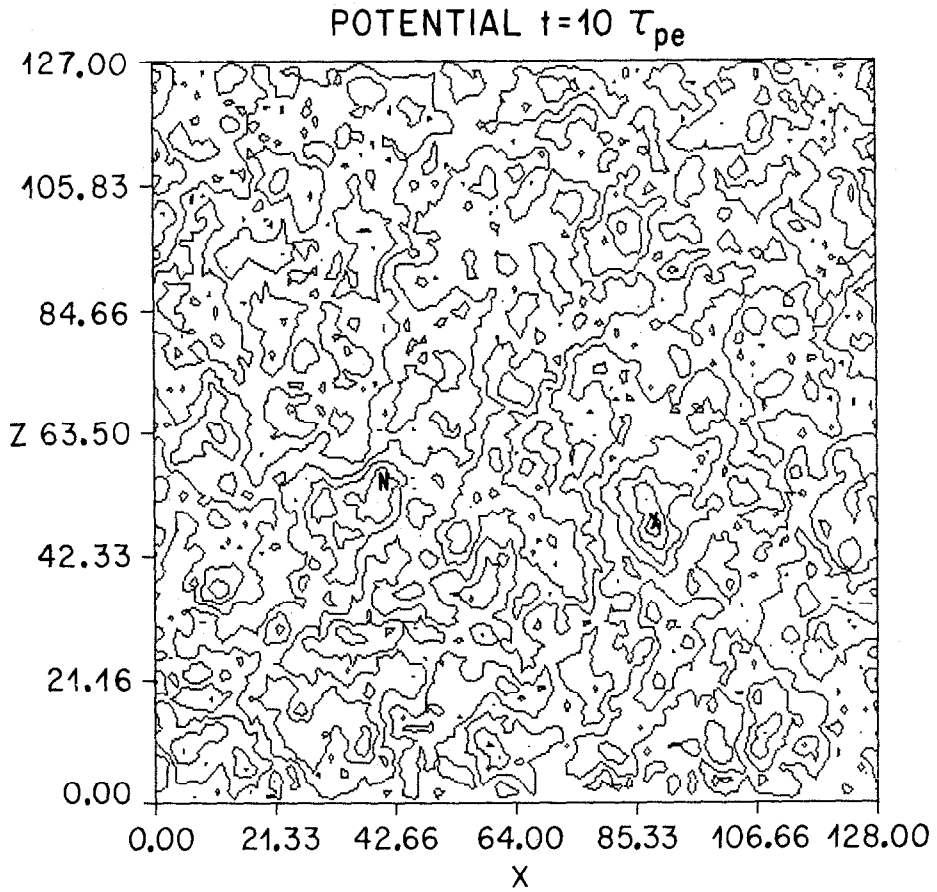

FIG. 1. Equipotential contours for a two-dimensional simulation of unmagnetized ions and strongly magnetized electrons. The magnetic field points toward the top of the figure. Periodic boundary conditions are assumed along the right- and left-hand boundaries, while the zero potential condition is imposed along the top and bottom boundaries. The position of the potential maximum and minimum is denoted by X and N, respectively. Distances are in grid units, and τ_{pe} is an electron plasma period.

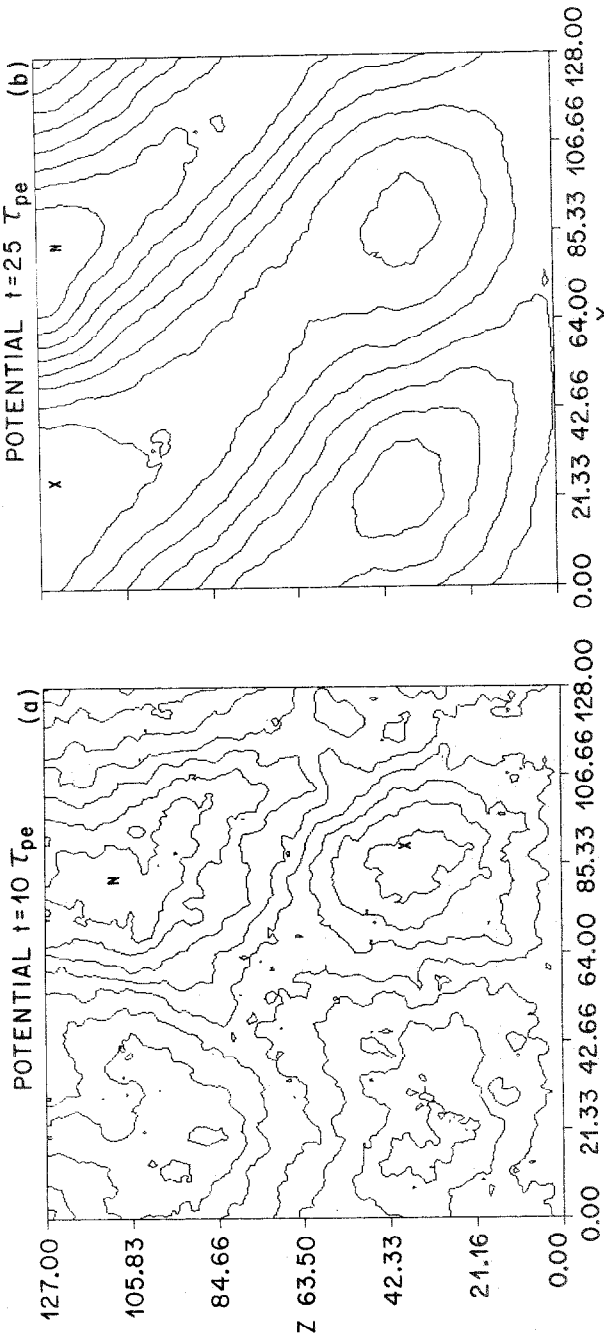

FIG. 2. Same as Fig. 1, except that along the top boundary, the zero normal derivative condition is imposed on the electric potential. (a) At the same time as the potential shown in Fig. 1. (b) At the end of the run.

domain. Since the electron and ion drifts were the same, no free energy was available for the excitation of instabilities. The electric field energy was about 2 % of the thermal energy of each species of particle, and the plasma showed no indication of instability.

Figure 2 shows equipotential contours of a run which is identical to that shown in Fig. 1, except that along the top boundary the conditions $\partial\phi/\partial z = 0$ as imposed. Figure 2a corresponds to the same time as Fig. 1. The large-scale structure in Fig. 2a in comparison to Fig. 1 is apparent, and the maximum potential differences generated are a factor of 3 larger than those in Fig. 1. Figure 2b shows a high degree of organization, dominated by large-scale structure, where the maximum potential differences are a factor of 12 greater than the potential differences in Fig. 1; and the electrostatic energy is 25 % of the total thermal energy. Examination of the time series for the potential at a given point revealed an oscillation at a frequency of $\omega = \omega_{pe}/\sqrt{2}$. The phase velocity of the wave was much larger than all particle speeds, and thus we identified the mode as the cold plasma oscillation

$$\omega^2 = \omega_{pe}^2 \cos^2 \alpha + \omega_{pi}^2. \tag{1}$$

The above relation holds for strongly magnetized electrons and unmagnetized ions; α is the angle between the magnetic field and the wave normal. The field energy grew at an approximately exponential rate between 12.5 and 25 τ_{pe}, with an e-folding rate of 0.19 τ_{pe}^{-1}.

Clearly, in both examples the particles contain no free energy. The fact that one run exhibited no unstable behavior, while the other run, shown in Fig. 2, did exhibit unstable behavior, indicates that the growth of instability must be attributed to the change in boundary conditions on the potential.

The purpose of this paper is to present a systematic analysis of the effects of boundary conditions on plasma behavior. The next section will present a conservation theorem which will form the basis of the analysis. The following section will present a one-dimensional theory of boundary-induced plasma instabilities, and Section 4 will describe some one-dimensional computer experiments which illustrate the theory. The final section will give some practical advice for avoiding the non-physical effects of boundary-induced instabilities.

2. Analysis of Boundary-Induced Instabilities

In this section, we shall derive a relation between the rate of change of field and of particle energy within a plasma in terms of energy fluxes across the boundaries surrounding the plasma. This will be done by differentiating with respect to time an expression for the sum of field and particle energies. The Vlasov and field equations will be used to convert the energy expressions into surface integrals.

In a simulation, the plasma is represented by a ditribution function of the type

$$f(\mathbf{x}, \mathbf{v}, t) = \sum_{k=1}^{P} S(\mathbf{x} - \mathbf{x}_k(t))\, \delta(\mathbf{v} - \mathbf{v}_k(t)), \tag{2}$$

where S is a particle shaping function, and the sum runs over all of the particles in the system. Actually, the details of the distribution function are not important for the arguments to be presented. This particular form was exhibited because it is a good representation of the type of distribution used in particle simulations. In what follows, we shall include magnetic as well as electrostatic energy, but the displacement current term in the equations describing the electromagnetic field will be neglected.

The total field and particle energy contained within a volume is given by

$$W = \int_V d^3r \left[\sum_j \int \frac{1}{2} m_i v^2 f_i d^3v + \frac{|\nabla\phi|^2}{8\pi} + \frac{B^2}{8\pi} \right], \tag{3}$$

where the sum over j represents the sum over particle species. The time rate of change of W is given by

$$\frac{dW}{dt} = \int_V d^3r \left[\sum_j \int \frac{1}{2} mv^2 \frac{\partial}{\partial t} f_i d^2v + \left(\nabla\phi \cdot \frac{\partial \nabla\phi}{\partial t} + \mathbf{B} \cdot \frac{\partial B}{\partial t} \right) \frac{1}{4\pi} \right], \tag{4}$$

where f satisfies the Vlasov equation

$$\frac{\partial f}{\partial t} = -\mathbf{v} \cdot \frac{\partial f}{\partial \mathbf{r}} - \frac{e}{m} \left[\left(\mathbf{E} + \frac{\mathbf{v}}{c} \times \mathbf{B} \right) \cdot \frac{\partial f}{\partial \mathbf{v}} \right]. \tag{5}$$

The expression for $\partial f/\partial t$ is substituted into (4) to calculate the rate of change of particle kinetic energy. First, we observe that

$$\int v^2 \left(\frac{\mathbf{v}}{c} \times \mathbf{B} \right) \cdot \frac{\partial f}{\partial \mathbf{v}} d^3v = 0. \tag{6}$$

The term involving the spatial derivative on f may be converted into a surface integral

$$\int_V d^3r \int \frac{1}{2} mv^2 \mathbf{v} \cdot \frac{\partial f}{\partial \mathbf{r}} d^3v = \oint \mathbf{F} \cdot d\mathbf{s}, \tag{7}$$

where the integral over $d\mathbf{s}$ is over the surface enclosing the volume, V, and $\mathbf{F}_j$ is the kinetic energy flux transported by the particles of species j,

$$\mathbf{F}_j = \int \frac{1}{2} m_j \mathbf{v} v^2 f_j d^3v. \tag{8}$$

The remaining term, and the one of most interest here, is that involving the electric field. We observe that

$$\int_V d^3r \sum_j e_j \int d^3v \frac{1}{2} v^2 \mathbf{E} \cdot \frac{\partial f_j}{\partial \mathbf{v}} = -\int_V \mathbf{E} \cdot \mathbf{j} d^3r, \tag{9}$$

where $\mathbf{j}$ is the electric current given by

$$\mathbf{j} = \sum_j e_j \int \mathbf{v} f_j d^3v. \tag{10}$$

At this point, it will be convenient to write $\mathbf{E}$ in terms of its irrotational and solenoidal parts,

$$\mathbf{E} = -\nabla\phi - \frac{1}{c}\frac{\partial \mathbf{A}}{\partial t}. \tag{11}$$

We can write, making use of Ampere's law

$$\frac{1}{c}\int_V d^3r \frac{\partial \mathbf{A}}{\partial t} \cdot \mathbf{j} = \frac{c}{4\pi}\oint \mathbf{E}_s \times \mathbf{B} \cdot d\mathbf{s} + \frac{1}{4\pi}\int_V \frac{\partial \mathbf{B}}{\partial t} \cdot \mathbf{B} d^3r. \tag{12}$$

The surface integral term is the Poynting flux through the surface, while $\mathbf{E}_s = -(1/c)\,\partial \mathbf{A}/\partial t$ refers to the solenoidal part of the electric field. Finally,

$$-\int_V d^3r \nabla\phi \cdot \mathbf{j} = -\oint \phi \mathbf{j} \cdot d\mathbf{s} - \frac{c}{4\pi}\int_V \frac{\partial \nabla\phi}{\partial t} \cdot \nabla\phi \, d^3r, \tag{13}$$

where use has been made of the equation for charge conservation, and of Poisson's equation. Incorporating these results into (9), our expression for the rate of change of plasma and field energy is now given by

$$\frac{dW}{dt} = -\oint \mathbf{F} \cdot d\mathbf{s} - \oint \phi \mathbf{j} \cdot d\mathbf{s} - \frac{c}{4\pi}\oint \mathbf{E}_s \times \mathbf{B} \cdot d\mathbf{s}. \tag{14}$$

Now, returning to the simulation examples displayed in Figs. 1 and 2, $E_s = 0$ and so the apparent culprit that led to the instability is the surface integral involving $\phi\mathbf{j}$. In the simulation leading to Fig. 1, ϕ was set to zero at two ends of the domain, and periodic boundary conditions were imposed along the other two sides so the surface integral was zero. In the example depicted in Fig. 2, ϕ at the top end was left to float, so $\phi\mathbf{j} \cdot d\mathbf{s}$ was non-zero at that end.

We note that as in the example described by Naitou *et al.* [4], a boundary-induced instability affected the interior of the domain. However, the example shown in Figs. 1 and 2 was a result of currents normal rather than tangential to this boundary.

Another difference is that in the Naitou *et al.* [4] example the instability was generated interior to, but near, the boundary, by boundary currents; whereas the example shown here was identified with a surface integral term.

3. Theory of the Boundary-Induced Instability

This section will develop a theoretical framework for a one-dimensional bounded plasma to gain insight on the process for excitation of the instability. As a model, we shall consider linear plasma oscillations in a bounded electron plasma in which the ions are assumed to form a uniform neutralizing background. The boundary conditions $\phi(0) = 0$ and $\phi'(L) = 0$ will be imposed.

We therefore seek linearized solutions to the equations

$$\frac{\partial f}{\partial t} + v\frac{\partial f}{\partial z} + \frac{e}{m}\frac{\partial \phi}{\partial z}\frac{\partial f}{\partial v} = 0, \tag{15}$$

and

$$\frac{\partial^2 \phi}{\partial z^2} = -4\pi e(n_0 - n_e), \tag{16}$$

therefore

$$f = f_0(v) + f_1(z, v, t) \tag{17a}$$

and

$$(n_e - n_0) = n_0 \int f_1 \, dv. \tag{17b}$$

The linearized Vlasov equation takes from

$$\frac{\partial f_1}{\partial t} + v\frac{\partial f_1}{\partial z} = -\frac{e}{m}\frac{\partial \phi}{\partial z}\frac{\partial f_0}{\partial v} \tag{18}$$

which has the solution

$$f_1 = g(t - z/v) - \frac{e}{m}\int_0^\infty d\tau \left.\frac{\partial \phi(z', t = \tau)}{\partial z'}\right|_{z' = z - v\tau} \frac{\partial f_0}{\partial v}. \tag{19}$$

particle distribution function. We then assume the potential can be expanded on terms of the complete set of basis functions

$$\left\{\sin\frac{(n + 1/2)\,\pi z}{L}\right\}$$

that satisfies the prescribed boundary conditions:

$$\phi(z, t) = e^{-i\omega t} \sum_{n=0}^{\infty} \phi_n \sin \frac{(n + 1/2)\,\pi z}{L}. \tag{20}$$

When this is substituted into (19) and the indicated integration carried out

$$\begin{aligned} f_1 = {} & \psi_0\, g_0(v)\, e^{-i\omega(t - z/v)} + \psi_L\, g_L(v)\, e^{-i\omega(t-(z-L)/v)} \\ & - \frac{e}{m} \frac{\partial f_0}{\partial v} e^{-i\omega t} \sum_n \frac{\phi_n k_n}{(\omega^2 - k_n^2 v^2)} [i\omega \cos k_n z + k_n v \sin k_n z], \end{aligned} \tag{21}$$

where $k_n = (n + 1/2)\,\pi/L$. The velocity distribution functions g_0 and g_L are the distribution functions of particles injected at $z = 0$ and L, respectively. The procedure for obtaining a dispersion relation is to integrate f_1 over velocities to obtain the perturbation number density $n_e - n_0$ of (17b). This, along with the expansion in (2) is substituted into the Poisson equation (16). The resulting expression is then multiplied by $\sin k_m z$ and integrated over the domain. The result is an infinite matrix equation in which the matrix elements are transcendental functions of the eigenvalue, ω. Although the procedure described above is reasonably straightforward, the task of finding eigenvalues to demonstrate instabilities is not.

Instead, we shall be content with a much more limited objective, namely, to show that, given either undamped or growing waves, the boundary term ϕj in (15) has a negative time average, signifying sustained electrical energy input into the plasma. To do this, we simply calculate

$$j = en_0 \int f_1 v\, dv \tag{22}$$

and multiply by the expression in (20). For definiteness, we assume f_0 in (21) to be of the form

$$f_0 = \left(\frac{m}{2\pi\theta}\right)^{1/2} e^{-m(v - v_0)^2/2\theta} \tag{23}$$

and g_0 to be of the form

$$\begin{aligned} g_0 &= \eta f_0 \qquad v \geqslant 0 \\ &= 0 \qquad v < 0 \end{aligned}$$

and similarly for g_L except that it is non-zero only for negative velocities, where n is a normalizing constant. The actual forms of g_0 and g_L are unimportant, because it can be shown that

$$J_0(z) = \int_0^{\infty} v g_0(v)\, e^{i\omega z/v}\, dv \tag{24}$$

decreases as an exponential function of $z\omega/\Delta v$, where Δv is the thermal spread in g_0. The distribution g_0 is assumed normalized such that $J_0(0) = 1$, and it is assumed that $L\omega/\Delta v \gg 1$ so that $J_0(L)$ is exponentially small. Since we are interested in evaluating the current only at $z = 0$ and L, it is not necessary to evaluate J_0 for all points in the interior of the domain. Similarly, we can omit the requirement to explicitly evaluate $J_L(z)$, where $J_L(L) = 1$, the boundary flux term at $z = L$. The resulting expression for the current density is therefore

$$\begin{aligned} j = {} & e\psi_0 J_0(z)\, e^{-i\omega t} + e\psi_L J_L(z)\, e^{-i\omega t} \\ & - \frac{n_0 e^2}{4\theta} e^{-i\omega t} \omega \sum_n \phi_n \frac{1}{k_n} \\ & \times \{i[Z'(\beta_n^+) + Z'(\beta_n^-)] \cos k_n z + [Z'(\beta_n^+) - Z'(\beta_n^-)] \sin k_n z\}, \end{aligned} \tag{25}$$

where $\beta_n^{\pm} = (\omega \pm k_n v_0)(m/2\theta)^{1/2}/k_n$, and Z' is the derivative of the plasma dispersion function.

At this point, we impose boundary conditions on the electron current. A common particle boundary condition is that particles which leave one end the domain are reinserted at the opposite end. This requires that

$$\psi_0 = -\frac{n_0}{4\theta} e\omega \sum_n \frac{\phi_n}{k_n} [Z'(\beta_n^-) - Z'(\beta_n^+)](-1)^n \tag{26a}$$

and

$$\psi_L = -i \frac{n_0}{4\theta} e\omega \sum_n \frac{\phi_n}{k_n} [Z'(\beta_n^+) + Z'(\beta_n^-)]. \tag{26b}$$

Although these expressions may be positive or negative, it should be remembered that they are first order quantities, which must be added to the steady zero order boundary fluxes to obtain the total flux. However, the steady zero order flux does not contribute to the long term average energy balance because this steady part of the flux, when multiplied by the oscillating ϕ averages to zero.

Finally, upon substituting (26) into (25) and multiplying it by the expression (20) for $\phi(z, t)$ and evaluating at $z = L$ and remembering that $J_0(L) \simeq 0$, the electric energy flux at $z = L$ is obtained

$$\begin{aligned} -j\phi\,|_{z=L} = {} & \left(\sum_{n'} \phi_{n'}(-1)^{n'}\right) \frac{n_0 e^2}{4\theta} \omega \\ & \times \left\{\sum_n i \frac{\phi_n}{k_n} [Z'(\beta_n^+) + Z'(\beta_n^-)] - \sum_n (-1)^n \frac{\phi_n}{k_n} [Z'(\beta_n^+) - Z'(\beta_n^-)]\right\}. \end{aligned} \tag{27}$$

There is no energy flux at $z = 0$ because $\phi(z = 0) = 0$.

In the runs depicted in Figs. 1 and 2 and the one-dimensional runs to be described below, the phase velocity of the wave far exceeds any particle velocities, so it is

appropriate to use the asymptotic expansion of the plasma dispersion functions for $\mathrm{Im}(\beta) \geqslant 0$, $Z'(\beta_n) \simeq \beta_n^{-2}$, then

$$-j\phi\,|_{z=L} = \left(\sum_{n'} \phi_{n'}(-1)^{n'}\right) \frac{n_0 e^2}{2m} \left\{\sum_n i\left[\frac{k_n\omega}{(\omega + k_n v_0)^2} + \frac{k_n\omega}{(\omega - k_n v_0)^2}\right]\phi_m \right.$$
$$\left. - \sum_n \left[\frac{k_n\omega}{(\omega + k_n v_0)^2} - \frac{k_n\omega}{(\omega - k_n v_0)^2}\right]\phi_n(-1)^n\right\}. \tag{28}$$

In the limit of zero drift, the second term in the curly bracket in (33) vanishes. The remaining term is a consequence of the particles that exit from the domain at $z = 0$ and are reinserted at $z = L$.

Making the assumption that the z-dependence of the eigenmode is dominated by the $\sin k_n z$ function (28) is approximated by

$$-j\phi|_{z=L} = i\frac{n_0 e^2}{m}\frac{(-1)^n}{\omega k_n}(k_n\phi_n)^2. \tag{29}$$

Since the wave energy is proportional to the square of the electric field, $(k_n\phi_n)$, it can be seen that the energy input term is largest for the lowest values of k_n. We further see that the real part of $-j(L)\,\phi(L)$ will be positive for $\mathrm{Im}(\omega) > 0$ only if n is even. Thus we would expect the mode corresponding to $n = 0$ mode to be the fastest growing, and likely the dominant mode. Further, since the real part of $-\phi(L)\,j(L)$ is largest for ω pure imaginary, we would expect purely growing modes. It is therefore likely that in this model, drift of the electrons would have little substantial effect on the character of the instability. For real frequencies the contribution of the second term will be positive only if v_0 is positive. Therefore, for positive v_0, the modes corresponding to n odd might also be excited.

4. One-Dimensional Numerical Examples

In order to more systematically investigate the effect of particle and potential boundary conditions, a one-dimensional plasma model containing 8192 electrons in a domain specified by 128 grid points is used. The ions are assumed to form a uniform neutralizing background. For each of the runs to be described, there are 32 time-steps per plasma period, and there are two grid points per Debye length. Table I lists the runs, according to the particle and field boundary conditions, and the drift velocities. Also listed is whether the simulation can be shown to be stable according to the criterion that

$$\frac{dW}{dt} = \phi(0)\,j(0) - \phi(L)\,j(L) = 0. \tag{30}$$

Parameters which indicate whether the plasma showed signs of instability, namely, the maximum values of the ratio of the field to particle kinetic energy and potential

TABLE I

Characteristics of One-Dimensional Simulation Runs

Run #	P.B.C.	ϕ B.C.	VD	STABLE?	Max(WE/K_E)	max($\Delta\phi$)
1	Periodic	Periodic	0	Yes	0.003	0.6
2	Reflecting	$\phi(0)=0$ $\phi'(L)=0$	0	Yes	0.004	1.1
3	Periodic	$\phi(0)=0$ $\phi'(L)=0$	0	No	0.035	10.8
4	Periodic	$\phi(0)=0$ $\phi(L)=0$	0	Yes	0.003	0.85
5	Reflecting	$\phi(0)=0$ $\phi(L)=0$	0	Yes	0.003	0.7
6	Periodic	$\phi(0)=0$ $\phi'(L)=0$	$+V_{th}$	No	0.014	7.0
7	Periodic	$\phi(0)=0$ $\phi'(L)=0$	$-V_{th}$	No	0.010	6.8
8	Periodic	$\phi(0)=0$ $\phi(L)=0$	$+V_{th}$	Yes	0.002	0.7

Note. P.B.C., ϕ B.C., VD stand for particle boundary conditions, potential boundary conditions, and drift velocity. The max stands for maximum value achieved during run of 16 plasma periods. WE/KE is the ratio of field to particle kinetic energy, and $\Delta\phi$ is the maximum potential difference across domain.

difference across the domain during the run, are also listed. Periodic boundary conditions on the particles means that particles which leave one end of the domain are reinserted at the other end with their velocities unchanged. Reflecting boundary conditions means that particles are reinserted at the same end they leave, but with a change in the sign of the particle velocity. This condition sets the boundary current to zero. Reflecting boundary conditions are not used when the plasma has a drift because that would set up interpenetrating beams which are unstable, even if (30) is satisfied. The plasma drift, when non-zero, is at the thermal speed.

Run #1 is stable by virtue of the periodic boundary conditions on both field and particles so that $j(0)\,\phi(0)=j(L)\,\phi(L)$. This combination is the most common type imposed on particle simulations because it is used to represent large, statistically

either $j\phi$ is zero on each boundary either because ϕ was clamped, or because reflecting boundary conditions on the particles are used.

It can be seen from a glance at Table I that those runs predicted to be stable by the criterion of (30) have a much lower ratio of electric field to kinetic energy and a much smaller potential across the domain. Those runs in which there is a drift, the drift energy is the same as the thermal energy, and the ratio of electric field to particle energy tends to be a factor of 2 lower than comparable examples with no drift. The time series of the potential at selected locations shows an almost sinusoidal

variation in all of the stable runs. Figure 3a shows a time series of the potential at a given point in the domain for Run #1, which is typical of all stable runs. For comparison purposes, Fig. 3b shows the electric field energy as a function of time. This shows an irregular low-level variation, which is also typical of the stable runs. Figure 3c shows a plot of the potential at the last time-step in the run. This is also typical of the stable runs.

Figure 4 shows data corresponding to those shown in Figure 3, except it is for Run #3 which is indicated to be not stable. Again, this is typical for all of the runs which are indicated in Table I as not being stable. Figure 4a shows a time series of the potential which exhibits a highly irregular variation. Note the much different scale than in Fig. 3a. Figure 4b shows the electrostatic energy which indicates large irregular variations. Analysis of the particle energy data indicates a 33% variation in particle energy during the run. The instability apparently grew and saturated within an electron plasma period. This very rapid growth is consistent with the results of the analysis of the previous section which indicates a positive imaginary frequency, i.e., exponential growth corresponding to n even modes. Figure 4c shows the potential as a function of z. This shows the strong dominance of te $n = 0$ member of the set of basis functions $\sin\{(n + 1/2)\,\pi z/L\}$. This is an extreme example, but typical of most of the profiles in all of the unstable runs, and is also consistent with the analytical results of the previous section.

The potential profiles of Runs #3, 6, and 7 were decomposed into the basis functions for purposes of comparison with the theory of the previous section. It was found that the basis function coefficient corresponding to $n = 0$ was usually a factor of 5 to 10 larger than the $n = 1$ coefficient, which was in turn about twice as large as the $n = 2$ coefficient. The higher order coefficients decreased monotonically. However, it was found that for Runs #3 and 7 that the $n = 0$ and $n = 1$ coefficients had nearly the same time series, within a constant multiplication factor, but that the $n = 2$ time series was not well correlated. This suggests that the $n = 1$ coefficient is part of the $n = 0$ eigenmode, but that a separate eigenmode corresponding to $n = 2$ may be excited independently. However, in Run #6, in which there was streaming in the positive direction, the time series for the first three coefficients is poorly correlated suggesting that modes corresponding to $n = 0$, 1, 2 are all independently excited. These results are all consistent with the analyses of the previous section which indicated that modes corresponding to only even n would be excited if the drift velocity were zero or negative and that excitation would occur for all modes for positive drift velocities. It is perhaps of interest to note that in Run #6 there was an increase in total energy during the first three plasma periods followed by a decrease to an energy considerably below the initial energy. Run #7 exhibited an increase in total energy by about 80%.

It should be kept in mind that we are making the approximation that the actual eigemodes are well represented by the basis functions. An even more questionable assumption is that the analysis is valid for only small-amplitude, linear, oscillations, but comparisons are being made to large-amplitude disturbances, where nonlinear effects are undoubtedly important. Hence the only claim that can be made for the

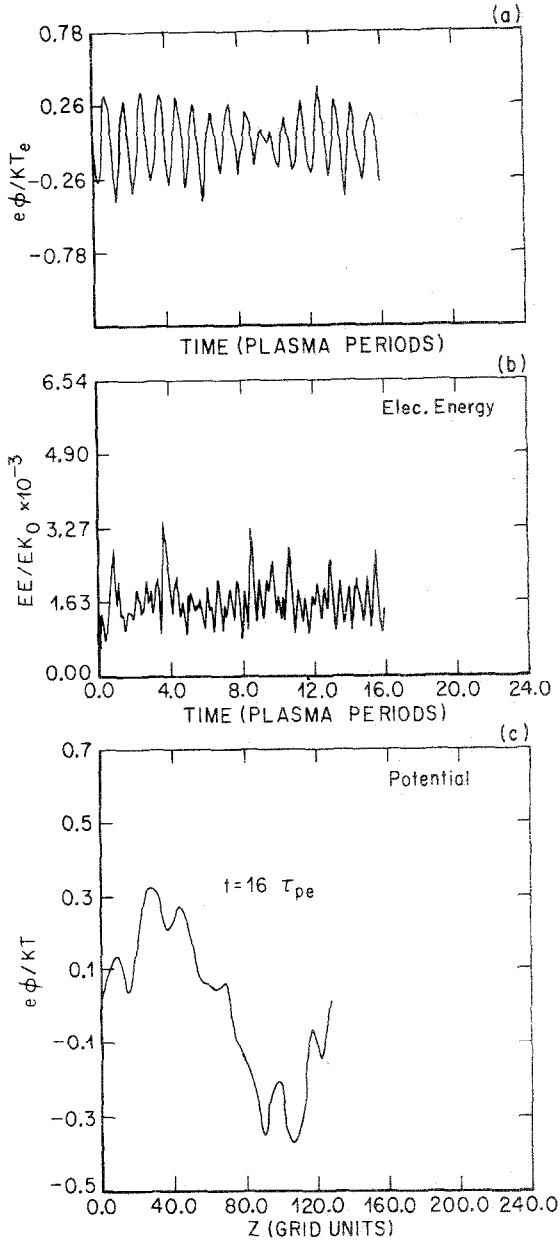

FIG. 3. Data from Run #1 of a one-dimensional simulation listed in Table I. Potential is in units of electron thermal energy. (a) A time series of the potential at a single point. (b) A time series of the electrostatic energy. (c) A profile of the potential at the end of the run.

comparisons between the analysis and numerical results is that the consistency lends support to the central thesis of this paper that suprious instabilites in simulation plasmas can be generated by boundary effects.

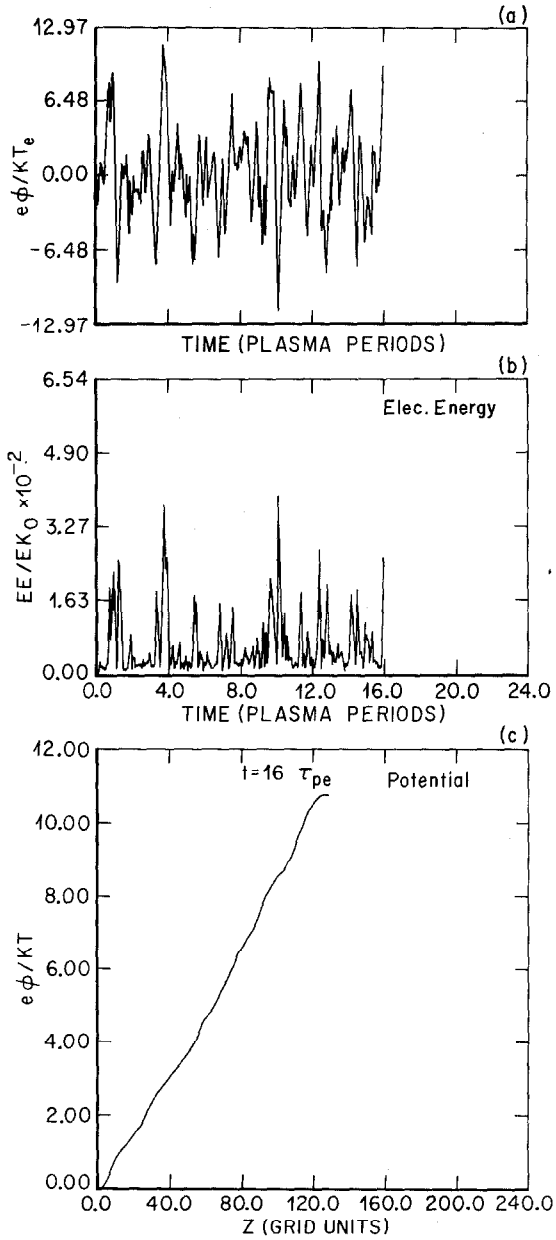

FIG. 4. Same as Fig. 3 except for Run #3 listed in Table I.

5. Discussion and Conclusion

This article has attempted to point out that spurious, non-physical instabilities may be generated in simulation plasmas if boundary conditions on the electric potential and particles are not handled properly. The analysis of Section 3 shows that the instability arises from the fact that particle fluxes across the boundaries of the simulation domain become correlated with electric potential variations in the simulation domain so that the term $j\phi$ may have a non-zero time average and contribute to a long-term buildup of wave energy in the plasma. The correlation of j and ϕ, if neither are deliberately clamped, arises because it is easier to write a code which maintains a constant number of particles in the simulation domain. Electric fields within a plasma will accelerate particles and alter the number of particles leaving the domain. If the particles that leave the domain are reinserted at the boundaries, then the particle flux, and hence the electric current will be correlated with the potential. This correlation is non-physical, so any instabilities arising from it are non-physical.

The most important practical results are contained in the middle term on its right-hand side of (15). Unless one can guarantee that the surface integral vanishes, an electrostatic code will likely be non-energy-conserving. If a non-energy-conserving simulation is desired, then special care must be taken to ensure that particle fluxes across the boundaries remain uncorrelated with potential variations to prevent the development of non-physical instabilities. In a magnetic code, where $\phi = 0$, energy conservation does not seem to require special handling of the particles because the Poynting flux term in (15) does not involve particle fluxes across the boundary.

Acknowledgment

This work was supported by the Atmospheric Sciences Section of the National Science Foundation under Grant ATM-7923614 and by the National Aeronautics and Space Administration under Grant NSG-7625.

References

1. C. K. Birdsall and A. B. Langdon, "Plasma Physics via Computer Simulation," Course Notes, Electrical Engineering and Computer Science Department, University of California, Berkeley, Calif., 1978.
2. J. S. Wagner, T. Tajima, J. R. Kan, J. N. Leboeuf, S.-I. Akasofu, and J. M. Dawson, *Phys. Rev.*
3. V. K. Decyk and J. M. Dawson, *J. Comput. Physics*, **30** (1979), 407.
4. H. Naitou, S. Tokuda, and T. Kamimura, *J. Comput. Physics*, **33** (1979), 86.
5. W. W. Lee and H. Okuda, *J. Comput. Physics*, **26** (1978), 139.